Mon. Not. R. Astron. Soc. **283,** 566–576 (1996)

Orbital decay of protostellar binaries in molecular clouds

U. Gorti and H. C. Bhatt

Indian Institute of Astrophysics, Bangalore 560034, India

Accepted 1996 July 5. Received 1996 June 26; in original form 1995 December 8

ABSTRACT

The evolution of a protostellar binary system is investigated while it is embedded in its parent molecular cloud core and is acted upon by gas drag as a result of dynamical friction. Approximate analytical results are obtained for the energy and angular momentum evolution of the orbit in the limiting cases, where the velocity is much smaller than, and much larger than, the velocity dispersion of the gas. The general case is solved numerically. Dispersion causes a decay of the orbit to smaller separations and the orbital eccentricity increases with time. Binary populations have been statistically generated and evolved for comparison with observations of the frequency distributions with periods of main-sequence (MS) and pre-main-sequence (PMS) binaries. Decay of the orbit as a result of dynamical friction can circumvent the problem of forming close binaries, as long-period binaries get dragged and evolve to shorter periods.

Key words: methods: analytical – binaries: close – binaries: general – stars: formation – ISM: clouds.

1 INTRODUCTION

Studies of star formation and early stellar evolution have, in the past, mainly concentrated on the processes involved in the formation of a single star. These have yielded a plausible sequence of events that lead to the formation of an optically visible young star from the gravitational collapse of a dense molecular cloud core (e.g. Shu, Adams & Lizano 1987). Observations of main-sequence stars and of present-day star formation sites, however, indicate that binary and multiple systems of stars are more common, and also that most star formation activity produces groups of stars rather than individual objects. Recent discoveries of large numbers of pre-main-sequence (PMS) binary systems, in both high-mass and low-mass star-forming regions, indicate that binaries are formed very early in the star formation process, probably even during the collapse phase itself. The formation of binaries thus appears to involve processes differing from, or additional to, those for a single star.

Observational studies of main-sequence binaries of F- and G-type dwarfs in the solar neighbourhood (Abt 1983; Duquennoy & Mayor 1991) indicate certain characteristic features such as a high fraction of stars in binaries (~ 70 per cent), a lognormal frequency–period distribution with a median at around 180 yr, a period–eccentricity relation, and a possible dependence on mass of the secondary mass distribution. These have provided constraints on theories of binary formation, which in recent times have been made more stringent by observations of PMS binaries themselves. The frequency distribution with period of PMS binaries appears also to have a single peak, but with seemingly a larger fraction of stars in binaries as compared with the MS stars. PMS binaries also exhibit a wide range of eccentricities and periods and are coeval. For a recent detailed review of PMS binary stars, refer to Mathieu (1994). (Also see reviews by Reipurth & Zinnecker 1993, Leinert et al. 1993, Bodenheimer 1992, and for theoretical aspects of binary formation, Pringle 1991 and Boss 1992). Theories for binary formation, thus in addition, must also explain the above observed characteristics of the binary population. There have been various mechanisms proposed to form binaries, which include (a) capture of individual stars by dissipation through tides, discs or residual gas, (b) fission of a collapsing rotating cloud core into two nuclei, (c) formation of a binary during hierarchical fragmentation of a collapsing cloud core and (d) instabilities in circumstellar discs. The observed smooth distribution of frequency with period for MS binaries with a single peak, suggests the presence of a characteristic scalelength and perhaps a single dominant mode for binary formation, if there were no further evolution of the binary orbit. Alternatively, different formation mechanisms acting on different scalelengths could all be equally important and would be expected to produce multiple peaks in the frequency distribution of periods. The

observed smooth distribution may then be due to an evolutionary process subsequent to formation that changes the binary orbital parameters.

As binaries form as condensations out of a molecular cloud, it is possible that their general properties depend on the physical properties of the parent molecular cloud/core. This is especially so, if the dominant formation mechanism is one of fragmentation (for example Henriksen 1991, Pringle 1991, Bodenheimer 1992, Boss 1992) where the properties of the fragments themselves are largely determined by the initial conditions in the collapsing cloud (e.g. Bodenheimer et al. 1980, Henriksen 1986, Henriksen 1991, Boss 1992). In fact, observations of PMS binaries in different star-forming regions do appear to indicate some differences in their features; the frequency of binaries may be lower in high-mass star-forming regions (binary-surveys of the Trapezium cluster region, Prosser et al. 1994) and there appears to be an excess of short-period binaries in the Ophiuchus–Scorpius region as compared with the Taurus–Auriga region (Mathieu 1992). Apart from an intrinsic difference in the nature of the protostellar cores formed subsequent to fragmentation, these objects probably undergo further dynamical evolution leading to an evolution of the binary properties as well. The protostellar binary is formed embedded in relatively massive amounts of distributed molecular cloud gas. Detection of binaries among protostars as young as 10^5 yr, and the fact that the observed frequency of PMS binaries appears to be as high as MS binaries, indicates that most binaries are formed during the early collapse phase. This suggests that a binary remains embedded in the cloud during much of its initial evolutionary period. Interactions with the residual gas in the cloud through various effects, can cause an orbital evolution of the protostellar binary. The effects of drag as a result of accretion on the orbital evolution of a binary system was studied in another context by Alexander, Chau & Henriksen (1976). They considered drag on the motion of one of the members, which is a compact star, moving in the extended envelope of its companion. In particular, they discussed in detail the effects of drag because of a stellar wind of constant radial velocity, emanating from the extended companion. On an estimation of the relevant time-scales, they concluded that gas drag causes a decay of the orbit and can also result in an increase of orbital eccentricity in some cases. In this paper, we study the influence of gas drag as a result of dynamical friction by the molecular cloud gas (Chandrasekhar 1943) on an embedded protostellar binary, and the time evolution of its orbital parameters. The effects of introducing the dissipative drag force are investigated both analytically and numerically. Dynamical friction may be regarded as arising from a density asymmetry of the surrounding medium in the wake of a moving object which tends to retard its motion by exerting a gravitational pull on the object (Binney & Tremaine 1987). Drag resulting from dynamical friction depends on the density and velocity dispersion of the ambient medium, and hence orbital evolution under different cloud conditions is considered. The evolution is also dependent on the binary parameters, such as the masses of the components, the initial separation and the eccentricity of the orbit. Statistically generated samples of binaries with a range of initial parameters are evolved in time to study changes in gross features of the binary population owing to dissipative drag forces. Approximate analytical results are presented in Section 2, the numerical methods are described in Section 3 and Section 4 contains a discussion of the results obtained. Section 5 discusses a statistical study of PMS binaries. Sections 6 and 7 contain a discussion on the implications of the results obtained for binary formation and the main conclusions, respectively.

2 EQUATIONS OF MOTION

We consider a uniform-density spherical cloud in which the protostellar binary system is embedded. The forces considered to be acting on each component of the binary system are (i) the gravity of the cloud, (ii) the gravitational force because of the other member and (iii) the dynamical friction force as a result of the ambient gas. All other forces are neglected. Thus the equations of motion in a coordinate frame centred on the cloud are,

$$\frac{\mathrm{d}^2\boldsymbol{r}_1}{\mathrm{d}t^2} = -4\pi G\rho\boldsymbol{r}_1 - \frac{Gm_2\boldsymbol{r}_{12}}{|\boldsymbol{r}_{12}|^3} - 4\pi \ln\Lambda_1 G^2 m_1 \rho \times \left(erf(X_1) - \frac{2X_1 \mathrm{e}^{-X_1^2}}{\sqrt{\pi}}\right)\frac{\boldsymbol{v}_1}{|\boldsymbol{v}_1|^3} \quad (1)$$

$$\frac{\mathrm{d}^2\boldsymbol{r}_2}{\mathrm{d}t^2} = -4\pi G\rho\boldsymbol{r}_2 + \frac{Gm_1\boldsymbol{r}_{12}}{|\boldsymbol{r}_{12}|^3} - 4\pi \ln\Lambda_2 G^2 m_2 \rho \times \left(erf(X_2) - \frac{2X_2 \mathrm{e}^{-X_2^2}}{\sqrt{\pi}}\right)\frac{\boldsymbol{v}_2}{|\boldsymbol{v}_2|^3} \quad (2)$$

where the last term in each of the above equations is the dynamical friction force. Here, m denotes the mass of the protostar, ρ is the density of the cloud and $\ln\Lambda$ denotes the Coulomb logarithm and is the ratio of maximum-to-minimum impact parameters. (The maximum impact parameter $\sim R$, the radius of the cloud, and the minimum impact parameter $= Gm/v^2$, so that $\Lambda \sim Rv^2/Gm$.) X is a dimensionless parameter equal to $v/\sqrt{2}\sigma$, where σ is the velocity dispersion of the cloud. The subscripts 1 and 2 in each case refer to the corresponding quantities for the two protostars, and $\boldsymbol{r}_{12}$ the relative position coordinate $\boldsymbol{r}_1 - \boldsymbol{r}_2$.

The cloud in which the binary system is embedded has a number density 10^6 cm^{-3}, is of size 0.3 pc, and has a velocity dispersion $\sigma = 2.3$ km s^{-1}. These conditions are typical of a protostellar environment (e.g. ρ Oph). The protostars are assumed to be of mass $m = 1$ M$_\odot$ each. For these values, and $v \sim \sigma$, $\ln\Lambda \sim 4$. In the following (Sections 2, 3 and 4), these are the values adopted for the different parameters, unless explicitly stated otherwise.

The equations are a set of coupled non-linear differential equations, an exact solution of which cannot be obtained. Since our interest is in the evolution of the binary, the orbital evolution can be equivalently described by the evolution of the angular momentum and energy of the system. These equations are also not easily solved for the general case. However, they may be approximately solved in the two limiting cases of (i) $v_{1,2} \ll \sigma$ where the dynamical friction term is proportional to the velocity $v_{1,2}$ and (ii) $v_{1,2} \gg \sigma$ when the drag is proportional to $1/v_{1,2}^2$. The equations can then be described in terms of the reduced mass of the system.

2.1 Case (i): $v_{1,2} \ll \sigma$

The velocities of the two masses can be expressed as the sum of the relative motion, v, and the centre of mass motion V. Thus,

$$v_1 = \frac{m_2 \boldsymbol{v}}{m_1+m_2} + \boldsymbol{V}; \qquad v_2 = \frac{-m_1 \boldsymbol{v}}{m_1+m_2} + \boldsymbol{V}. \tag{3}$$

From equations (1), (2) and (3), with the dynamical friction term now given by $-\eta m_i \boldsymbol{v}_i$ for each particle, we get

$$\frac{\mathrm{d}^2\boldsymbol{r}}{\mathrm{d}t^2} = -4\pi G\rho \boldsymbol{r} - \frac{G(m_1+m_2)\boldsymbol{r}}{|\boldsymbol{r}|^3} - \eta \frac{m_1 m_2}{m_1+m_2} 2\boldsymbol{v} - \eta(m_1-m_2)\boldsymbol{V} \tag{4}$$

where $\eta = 16\pi^2 G^2 \ln \Lambda \rho / [3(2\pi\sigma^2)^{3/2}]$. The last term is neglected and the rate of change of angular momentum can then be written as

$$\frac{\mathrm{d}\boldsymbol{L}}{\mathrm{d}t} = \mu \boldsymbol{r} \times \frac{\mathrm{d}\boldsymbol{v}}{\mathrm{d}t} = -2\mu\eta \boldsymbol{L} \tag{5}$$

where μ is the reduced mass. Therefore,

$$\boldsymbol{L} = \boldsymbol{L}_0 \mathrm{e}^{-2\mu\eta t}. \tag{6}$$

The time rate of change of energy and angular momentum of the orbit can be obtained in a more general manner by rewriting the equations in a Lagrangian formulation. The dissipative drag force can be expressed as the velocity gradient of a 'dissipative function', $\mathcal{F}$ (in the limit $v_{1,2} \ll \sigma$) given by

$$\mathcal{F} = \eta \mu^2 v^2. \tag{7}$$

The rate of change of angular momentum is obtained from one of the Lagrange equations, and is equal to $-2\mu\eta L$, as was already obtained in equation (5). The rate of change of energy is given by (refer to, for example, Goldstein 1977)

$$\frac{\mathrm{d}E}{\mathrm{d}t} = -\sum \frac{\partial \mathcal{F}}{\partial \dot{q}_j} \dot{q}_j = -2\eta\mu^2 v^2 \tag{8}$$

where $\dot{q}_j$ represents the generalized velocities. It can be assumed that the system evolves quasi-virially, such that the virial theorem always holds during the motion. The total energy, E, is thus equal to one-half the kinetic energy, and for a circular orbit, the velocity can be expressed in terms of the total energy as $v^2 = -2E/\mu$. Thus,

$$\frac{\mathrm{d}E}{\mathrm{d}t} = 4\eta\mu E \quad \text{and} \quad E = E_0 \mathrm{e}^{4\eta\mu t}. \tag{9}$$

The equations have also been numerically solved (see Section 3) and a comparison with the analytical solutions (equations 5 and 8) shows that though the equations have been solved for the circular orbit, they approximate reasonably well for higher-eccentricity orbits. The rate of change of eccentricity with time cannot, however, be obtained from the present solutions, as the orbit always remains circular. Fig. 1 shows the time evolution of angular momentum, energy and semimajor axis of the binary system. Here, $\eta = 1.19$ and $\mu = 0.5$.

2.2 Case (ii): $v_{1,2} \gg \sigma$

For velocities large compared with the local velocity dispersion of the background, the dynamical friction force is proportional to $1/v_{1,2}^2$ and the equations of motion are

$$\frac{\mathrm{d}^2\boldsymbol{r}}{\mathrm{d}t^2} = -4\pi G\rho \boldsymbol{r} - \frac{G(m_1+m_2)\boldsymbol{r}}{|\boldsymbol{r}|^3} - \tilde{\eta}\left(\frac{m_1 \boldsymbol{v}_1}{|\boldsymbol{v}_1|^3} - \frac{m_2 \boldsymbol{v}_2}{|\boldsymbol{v}_2|^3}\right), \tag{10}$$

where $\tilde{\eta} = 4\pi \ln \Lambda G^2 \rho$. For simplicity, it is assumed that the two masses are equal and $v_1^3 = v_2^3 \approx (v^2/4 + V^2)^{3/2}$ so that equation (10) reduces to

$$\frac{\mathrm{d}^2\boldsymbol{r}}{\mathrm{d}t^2} = -4\pi G\rho \boldsymbol{r} - \frac{2Gm\boldsymbol{r}}{|\boldsymbol{r}|^3} - \frac{\tilde{\eta} m \boldsymbol{v}}{(v^2/4+V^2)^{3/2}} \tag{11}$$

where m represents the mass of the protostars. The dissipative function $\mathcal{F}$ is thus

$$\mathcal{F} = \frac{2\tilde{\eta} m^2}{(v^2/4+V^2)^{1/2}}. \tag{12}$$

The rate of change of energy is again given by equation (8) and is integrated by assuming that the velocity of the centre of mass is a constant, and that virial equilibrium always holds. Therefore, for a circular orbit,

$$\frac{2}{3}\sqrt{E_k - E}\,(4E_k - E) + E_k^{3/2} \ln \frac{\sqrt{E_k - E} - \sqrt{E_k}}{\sqrt{E_k - E} + \sqrt{E_k}} = 2\tilde{\eta} m^{5/2} t + c \tag{13}$$

where E_k is equal to mV^2 and c is the constant of integration, to be determined from the initial conditions. The equation of motion for a particle orbiting a central point mass was studied by Hoffer (1985) who developed approximate expressions for the evolution of the semimajor axis of the orbit. It can be easily shown that the above equation corresponds to Hoffer's solution in the limit of vanishing E_k. The angular momentum equation can be obtained as above,

$$\frac{\mathrm{d}\boldsymbol{L}}{\mathrm{d}t} = -\frac{\tilde{\eta} m \boldsymbol{L}}{(v^2/4+V^2)^{3/2}}. \tag{14}$$

This can be integrated for a circular orbit to give the evolution of angular momentum

$$\left(-\frac{4V^2}{3} - \frac{k^2}{12L^2}\right)\left(\frac{k^2}{4L^2} + V^2\right)^{1/2} + V^3 \ln \left[V^2 L + LV\left(\frac{k^2}{4L^2} + V^2\right)^{1/2}\right] = -\tilde{\eta} m t + c \tag{15}$$

where k is equal to Gm^2 and c is a constant to be determined from the initial conditions. The equations (13) and (15) are transcendental in nature and the energy and angular momentum cannot be easily expressed as explicit functions of time. The nature of the evolution can, however, be inferred. Initially, both energy and angular momentum are

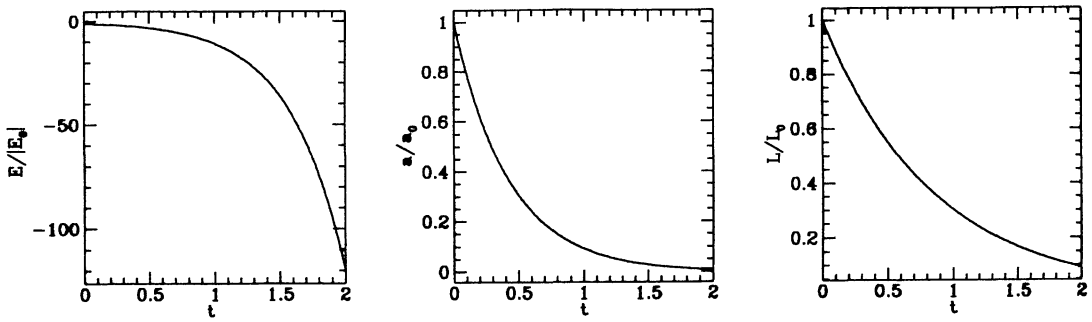

Figure 1. The energy, the semimajor axis and the angular momentum are plotted against time, scaled by their corresponding initial values. Here $\eta = 1.19$ and $\mu = 0.5$. (Case 1: $v \ll \sigma$.)

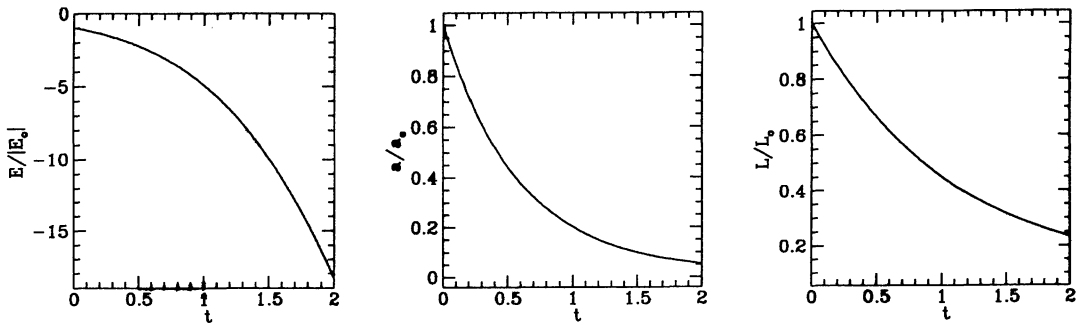

Figure 2. The energy, the semimajor axis and the angular momentum are plotted against time, scaled by their corresponding initial values. $\tilde{\eta}$ corresponds to a cloud number density of 10^6 cm^{-3}, $m = 1$ M$_\odot$, and $V = \sigma = 2.3$ km s^{-2}. (Case 2: $v \gg \sigma$.)

exponential functions of time with a time-scale of the order $V^3/2\tilde{\eta}m$ and $V^3/\tilde{\eta}m$ respectively. For typical cloud conditions surrounding a protostar, with densities $\sim 10^6$ cm^{-3} (for example ρ Oph), and for $V \sim \sigma$, these time-scales are of the order of a few 10^5 yr. As the binary loses kinetic energy, the protostars fall in and become more tightly bound. The relative velocity of the binary thereby increases and change in energy and angular momentum of the binary is no longer exponential, but slower. At later times (when the relative velocity $v \gg V$, the centre-of-mass velocity), the energy varies as $\approx t^{2/3}$ and angular momentum as $\approx t^{1/3}$. Fig. 2 shows the variation of energy, angular momentum and semimajor axis of the binary system with time (where V has been taken equal to σ). η corresponds to a cloud number density of 10^6 cm^{-3}, and time is in units of 10^6 yr.

3 NUMERICAL SOLUTIONS

The equations governing the motion of the binary can be solved only in the limiting cases, where the dynamical friction term reduces to a simple form, and by making certain approximations. To study the complete evolution of the binary system, and to check the validity of the above derived expressions, equations (1) and (2) have been solved exactly using numerical methods. Also, the above expressions do not yield the variation of eccentricity with time, as it has been assumed that the orbit is always circular. The eccentricity of the orbit increases or decreases with time, depending on the relative rates of change of energy and angular momentum. Though dissipative forces are in general believed to circularize orbits, this is not necessarily so, one such exception being the drag arising from dynamical friction (e.g. Alexander et al. 1976 and Hoffer 1985). The numerical solutions allow a study of the eccentricity variation with time and also a more exact investigation of the other orbital parameters. The problem essentially involves two very different time-scales, one being the period of the binary, which may be of the order of years, and the other the drag time-scale which can be estimated to be of the order of $\sim 10^{5-6}$ yr, for usual protostellar cloud parameters. Thus the orbit has to be typically integrated over a few 10^6 periods and, to meet requirements of accuracy, forces are evaluated about a thousand times for each orbit. In order to check the accuracy of the integration scheme to be adopted, the binary is first evolved in the absence of drag for about 10^6 yr. Ideally, energy conservation is to be expected, which is not in general achieved by standard methods of integration that use a variable time-step. Ensuring energy conservation by choosing a constant time-step criterion (and thus a time-symmetric integrator) turns out to be prohibitively expensive and we adopt the prescription by Hut, Makino & McMillan (1995) for a time-symmetrized leapfrog with a variable time-step. The second-order method has been chosen over the fourth-order Hermite integrator as the latter has proved less economical for the present problem. The symmetrized leapfrog integrator involves the use of an implicit time-step criterion which preserves the time-symmetry of the original equations and excellent energy conservation (with the exclusion of drag) is obtained. The orbits are then integrated including the drag term in the forces.

Fig. 3 shows the variation in time of energy, angular momentum, eccentricity and semimajor axis, for an orbit

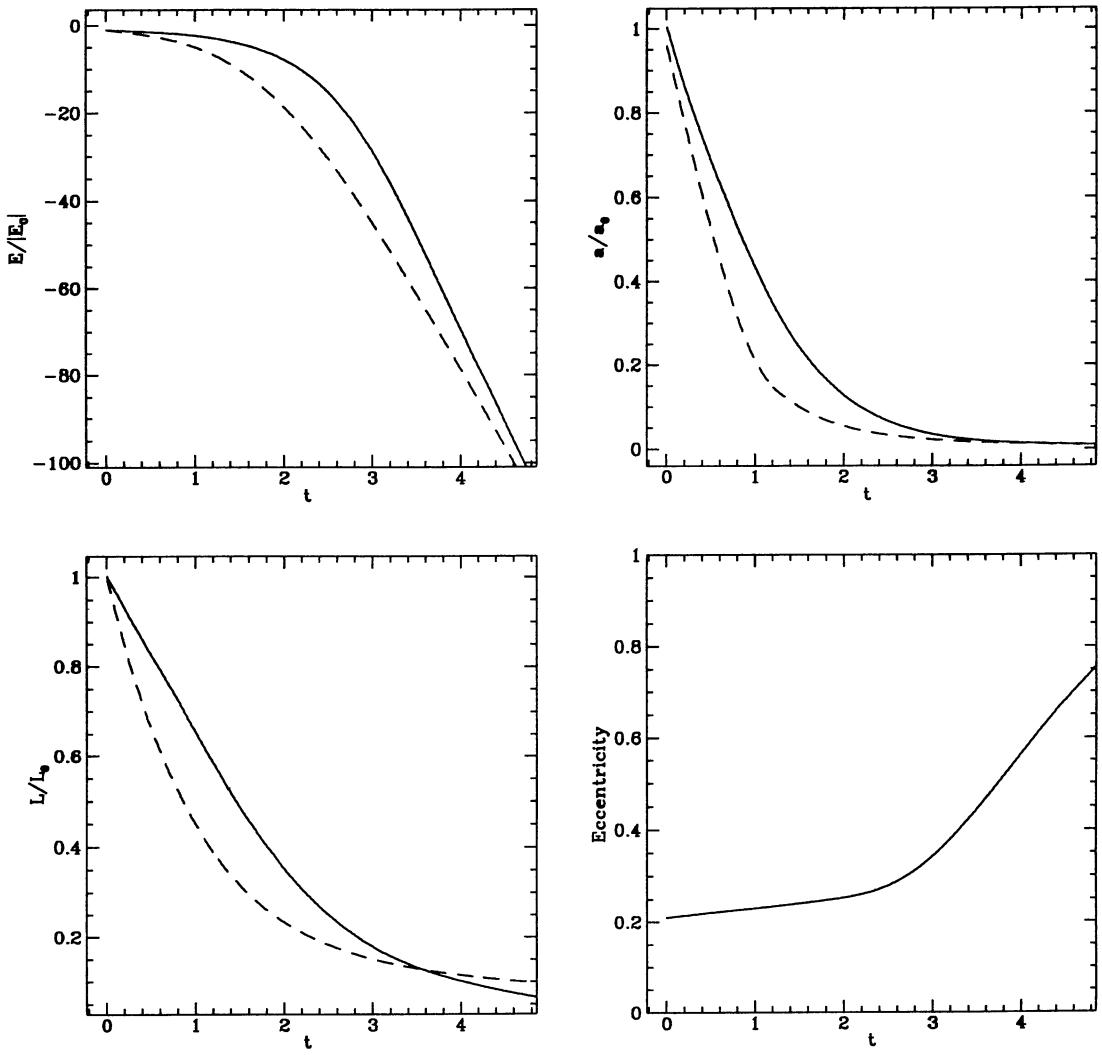

Figure 3. The energy, the semimajor axis, the angular momentum and the eccentricity are plotted against time. The solid lines correspond to the numerical result and the dashed lines to the analytical approximation (ρ corresponds to a cloud number density 10^6 cm^{-3}, $m_1 = m_2 = 1$ M$_\odot$, and $\sigma = 2.3$ km s^{-1}. Initially, $a = 1200$ au and $e = 0.2$).

with an initial semimajor axis of 1200 au and eccentricity, 0.2. Also shown superposed on these plots are the corresponding analytical solutions (for the case $v_{1,2} \gg \sigma$). It can be seen that there is reasonable agreement between the two, even though the orbit is not circular.

4 EVOLUTION OF A BINARY IN A CLOUD

As seen above, the predominant effect of the drag force on the binary is to shrink the orbit to smaller separations. The extent to which the orbit shrinks in a given period of time depends on the initial separation of the binary components. The initial semimajor axis of the binary determines the initial relative velocity, and hence the magnitude of the drag term in the force initially. As the masses lose energy and angular momentum and spiral in, their orbital separation decreases and there is an increase in the magnitude of their relative velocity. If the initial velocity is less than the gas velocity dispersion σ, then the drag force increases in magnitude in the beginning as v and decreases later as $1/v^2$. Thus, there is an initial rapid decay of the orbit and as the relative velocity increases, drag decreases and the decay is slower. Fig. 4 shows the evolution of the semimajor axis for different initial separations during a fixed interval of time. The initial eccentricity of the orbit was 0.2. The cloud in which the protostellar binary is embedded is assumed to be of constant number density (10^6 cm^{-3}) and with a velocity dispersion of 2.3 km s^{-1}. These parameters are typical of the environment of protostars and have been chosen to comply with observations of the prototypical star-forming cloud core, ρ Oph. It is seen that the time-scale for a decrease in the semimajor axis by a factor of two, $t_{1/2}$, is about a few 10^5 yr.

A distinct feature of drag resulting from dynamical friction is that orbits get increasingly more eccentric with time. This implies that the fractional loss of angular momentum exceeds that of energy. The eccentricity increases with time and gradually tends towards one. The increase of eccentricity with time as a result of dynamical friction was commented on by earlier authors (Alexander et al. 1976; Hoffer

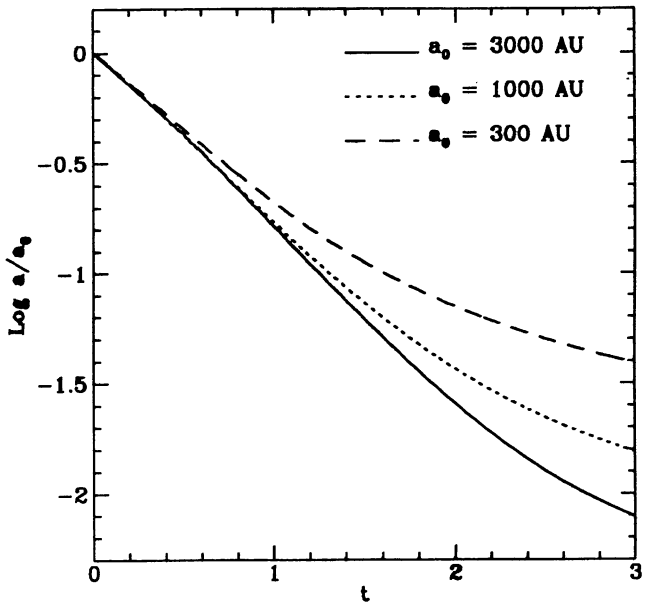

Figure 4. Evolution of the semimajor axis for different initial separations. Time is plotted in units of 10^6 yr ($m_1 = m_2 = 1$ M$_\odot$, and the initial eccentricity of the orbit is 0.2).

1985). We have studied eccentricity variations for differing initial eccentricity and Fig. 5 shows the initial and final eccentricity for an orbit with the same initial separation of 1000 au, after 10^6 yr. Also shown are the changes in angular momentum and energy with time. As is to be expected, loss of angular momentum is greater for orbits with higher eccentricity. The increase of eccentricity with time indicates that binary systems that have evolved in the presence of gas and hence suffered drag because of it, must lie on high-eccentricity orbits in general. While this may be so for orbits with long periods and hence larger separations, it need not hold for the shorter period binary systems. It is believed that almost all young protostars are accompanied by massive circumstellar discs, with typical extents of ~ 100 au (Strom, Edwards & Strutskie 1993). Therefore, for separations much shorter than these, the presence of the discs has to be taken into account for a more realistic analysis. It is not clear how dissipation caused by discs affects the eccentricity of the orbit, though at very short periods, tidal forces may rapidly tend to make the orbits more circular (Clarke 1992). As circumstellar discs have not been included in our present analysis, we have not considered the evolution of short-period binaries, as we believe that the effects of discs on the binary orbit is probably more prominent at these separations.

The effects of variation in cloud gas density can be assessed easily from equations (8), (10) and (11). The relevant time-scales vary inversely with density, and the evolution of the semimajor axis for three different cloud densities (with $\sigma = 2.3$ km s^{-1}), is shown in Fig. 6. The evolution for different gas velocity dispersions depends on the velocity of the binary and hence on the separation. Fig. 6 also shows the semimajor axis plotted against time for different velocity dispersions. The cloud density has been kept constant at $\sim 10^6$ cm^{-3}. The drag force depends sensitively on the velocity dispersion, and is greater for lower velocity dispersions. This implies that evolution of binaries subsequent to formation may, in general, be different for different clouds (with differing velocity dispersions or differing densities). There seems to be tentative observational evidence for differences in the frequency of short-period binaries in ρ Oph and Taurus–Augiga clouds. If the observed excess of closer binaries in ρ Oph is not because of a larger incidence of formation, evolution of PMS binaries in the presence of drag could be a possible explanation. ρ Oph has a lower velocity dispersion and a higher average gas density as compared with the Taurus–Auriga star-forming region, and hence a drag force of greater magnitude. This implies that evolution to shorter orbital separations is faster in ρ Oph and it is more likely to contain short-period PMS binaries.

It is to be noted that although only the dissipative effects of dynamical friction have been considered here, in principle, other forces could also drag the orbital evolution. For close binaries, discs and tidal torques provide active dissipative agents in addition to dynamical friction and are probably more important. Ram pressure resulting from the surrounding gas is another potential source of drag, and for self-gravitating objects like protostars, is similar in form to the dynamical friction term (in the limits of large velocity), except for being a factor of $\ln \Lambda$ lower in magnitude. The results derived here therefore apply equally well for ram pressure deceleration as well, but on longer time-scales.

5 STATISTICAL STUDIES OF PMS BINARIES

High-resolution techniques and better infra-red detectors have in recent times enabled the detection of large numbers of PMS binaries covering a wide range of periods. A comparison with observations of main-sequence (MS) binaries can thus be made and it is found that the fraction of PMS stars in binary systems is equal to or even larger than the frequency of MS binaries (~ 60–70 per cent). The periods of MS binaries form a smooth distribution in the range $0 < \log P(\mathrm{d}) < 9$, with a maximum at around 180 yr. The eccentricities span a wide range and only the shortest period orbits are circular. The masses of the primary and secondary are probably uncorrelated and are consistent with a random pairing from an initial mass function (Duquennoy & Mayor 1991). Periods of PMS binaries within the range observed appear to follow a similar distribution as that of the MS binaries. PMS binary orbits also have a range of eccentricities. Since drag affects the orbital evolution of a binary system as discussed above, it is to be expected that this will be manifest in the observed properties of PMS and MS binaries. In order to investigate the effects of gas drag on the class of PMS binaries as a whole, statistical samples of binary systems are generated and evolved in time. The initial conditions and assumptions made are as follows:

(i) The masses are determined from a Salpeter initial mass function ($\mathrm{d}N/\mathrm{d}M \propto M^{-2.35}$) within the range 0.5 to 5 M$_\odot$. Binaries are formed by randomly pairing two masses.

(ii) The eccentricities are random and constrained within the interval 0–0.8. Higher eccentricity orbits were not con-

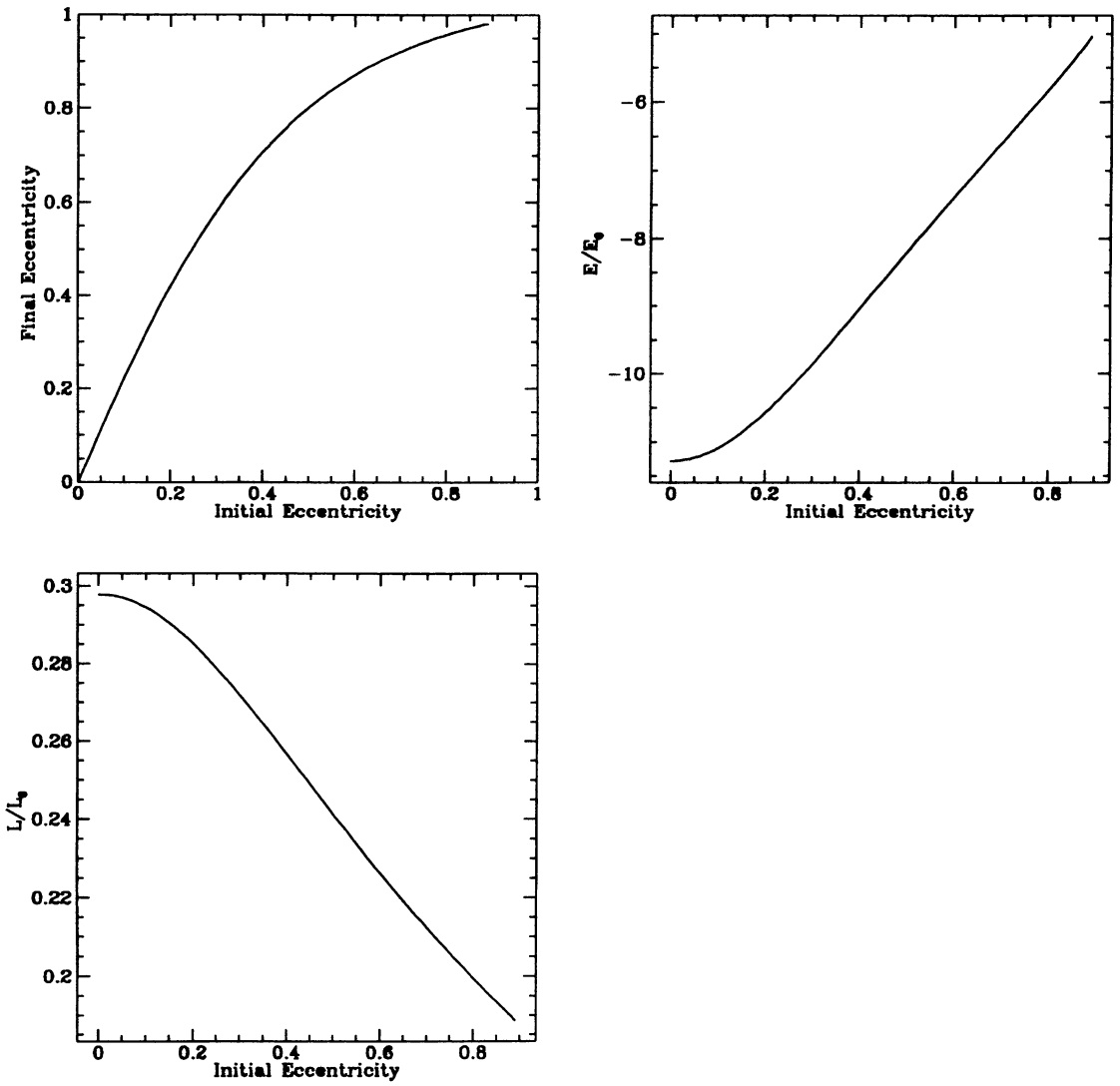

Figure 5. For different initial eccentricities of an orbit with the same initial separation, the eccentricity, the energy and the angular momentum after a fixed interval of time are shown. ($a = 1000$ au, and the other parameters have the same values as in Fig. 3.)

sidered because of difficulties in maintaining the accuracy during numerical integration.

(iii) The separations (and hence periods) of the entire sample follow an assigned distribution. Two such initial distributions were considered, one where the number of binaries *per separation interval* are equal (case I) and another where the number of binaries are equal *per logarithmic separation interval* (case II).

(iv) For each of the two cases, the assignment of a separation (semimajor axis) drawn from the specified distribution above, to a particular binary, is random. The separations are all constrained to lie within the range 100 to 10^4 au. The lower limit has been somewhat arbitrarily chosen and corresponds to the typical size of a protostellar disc, beyond which the disc is expected to significantly influence the orbital evolution. The upper limit corresponds to an average expected separation for protostars in a clustered environment, beyond which the binary may not remain bound.

(v) The binary is given a random position in the uniform density cloud (of density 10^6 cm^{-3} and velocity dispersion 2.3 km s^{-1}) and assigned a velocity v with an arbitrary direction. The magnitude of the velocity is determined by $v^2 = 4\pi G\rho R^2/3$, where R denotes the position of the binary.

The sample consists of 100 binaries for the case with an equal number per separation interval (case I) and 70 binaries for the case with equal number of binaries per logarithmic separation interval (case II). Each binary orbit is integrated in time for about 5×10^6 yr. The frequency distribution as a function of period at different instances of time for case I is shown in Fig. 7. The initial distribution is constant with separation, as shown in panel (a). As the drag force varies as the inverse square of the velocity, binaries with larger separations (and smaller velocities) suffer greater drag and lose energy at a higher rate as compared with the higher velocity binaries at shorter periods. The frequency distribution gradually gets altered and a peak appears, which gets more pronounced at later times. The

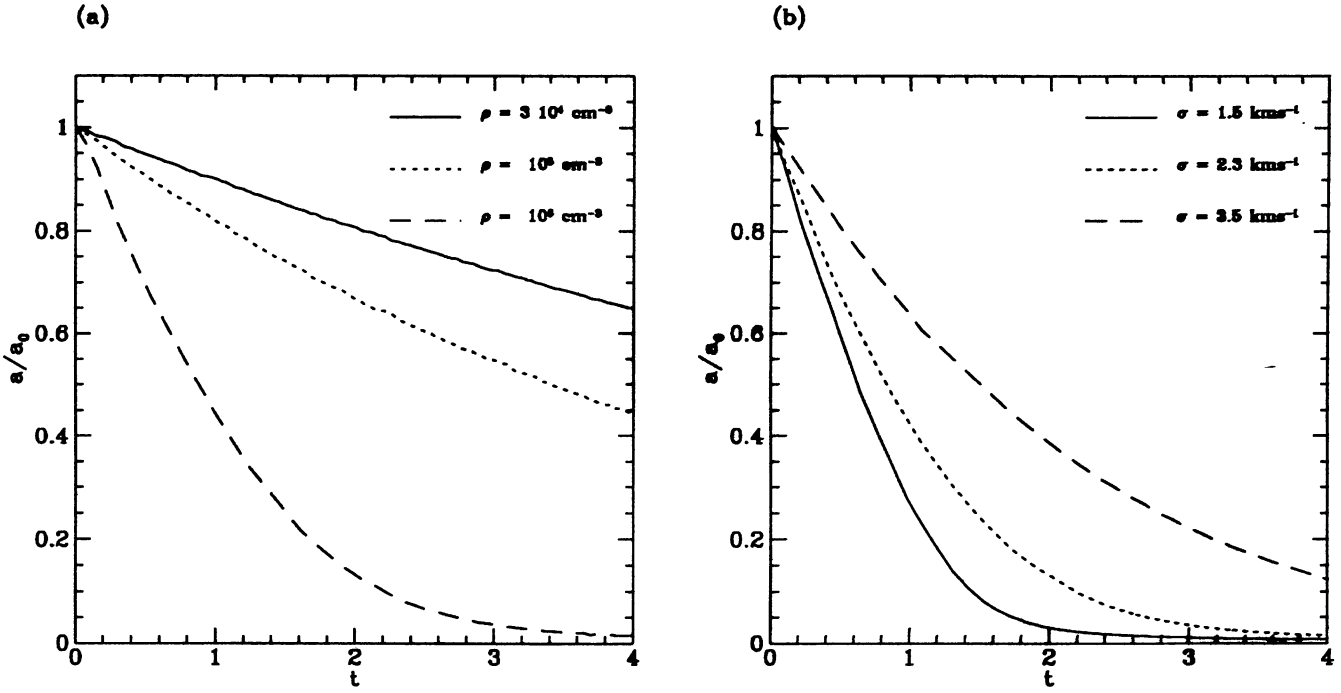

Figure 6. Evolution of the semimajor axis of a binary for different cloud densities [panel (a)] and velocity dispersion of gas in the cloud [panel (b)]. Time is in units of 10^6 yr. (The other parameters have the same values as in Fig. 3.)

position of the peak slowly shifts towards shorter periods if the evolution is allowed to proceed for longer times. For an initial distribution that is constant in equal logarithmic intervals of separation, the frequency distribution also gets gradually altered as shown in Fig. 8. A distinct peak in the frequency distribution appears at later times than in case I probably because of the presence of a comparatively larger number of short period binaries which evolve more slowly.

The observed maximum in the frequency distribution with period can perhaps possibly be explained as an effect of gas drag (or other dissipative forces) which determines the initial evolution of a binary while still embedded in the molecular cloud. The position of the maximum then depends mainly on the cloud parameters and to a much lesser extent on the duration of the embedded phase of a typical binary system. The observed peak in the MS binary distribution would then be representative of the typical or average cloud conditions in the Galactic star-forming environment.

The eccentricity of a binary acted upon by dynamical friction increases with time. This implies that binary orbits that have decayed to shorter periods are also more eccentric. Observations of MS binaries seem to show the reverse trend, with close binaries lying on nearly circular orbits. It is believed that for very close binaries, tidal forces rapidly tend to circularize the orbits (e.g. Mathieu 1994). The trend towards low eccentricities is however seen only for orbits with periods shorter than ~ few 100 d, and our analysis does not extend to such short-period binaries. Fig. 9 shows the observed eccentricities of MS binaries and those from the above samples, plotted against the period of the orbit for the overlapping range of periods ($3.5 < \log P\,(\mathrm{d}) < 5$. There is a slight tendency for the shorter period orbits to be more eccentric, as is expected. However, within the range of periods observed, there is no obvious contradiction between the results obtained here and observations.

6 IMPLICATIONS FOR BINARY FORMATION

The presence of a peak in the frequency distribution with separation for MS and PMS binaries suggests the existence of a preferred scalelength for the formation of binaries. Existing mechanisms for binary formation include fragmentation, fission, capture processes and instabilities in discs. Of these, fragmentation is currently believed to be the primary formation process (see reviews by Bodenheimer 1992, Pringle 1991, Boss 1992) where the protostar fragments during the isothermal collapse phase or alternatively where the binary is formed as a result of a hierarchical fragmentation process (Henriksen 1986). The frequency distribution arising from fragmentation is not well-determined (Boss 1992) but formation of binaries with larger separations is easier or more favoured than the formation of close binaries (Bodenheimer 1992). Decay of the orbit as a result of dynamical friction can circumvent the problem of forming close binaries, as long-period binaries get dragged and evolve to shorter periods.

If all (or any other) of the above mentioned mechanisms are equally important for the formation of binaries, there are intrinsically different scalelengths involved in each case (e.g. the separation of a binary cannot be much larger than the extent of the disc if the binary forms by gravitational instabilities in a disc). It is then very unlikely for the initial frequency distribution to be a uniform function of period. In such a case, dissipation of energy because of drag may serve

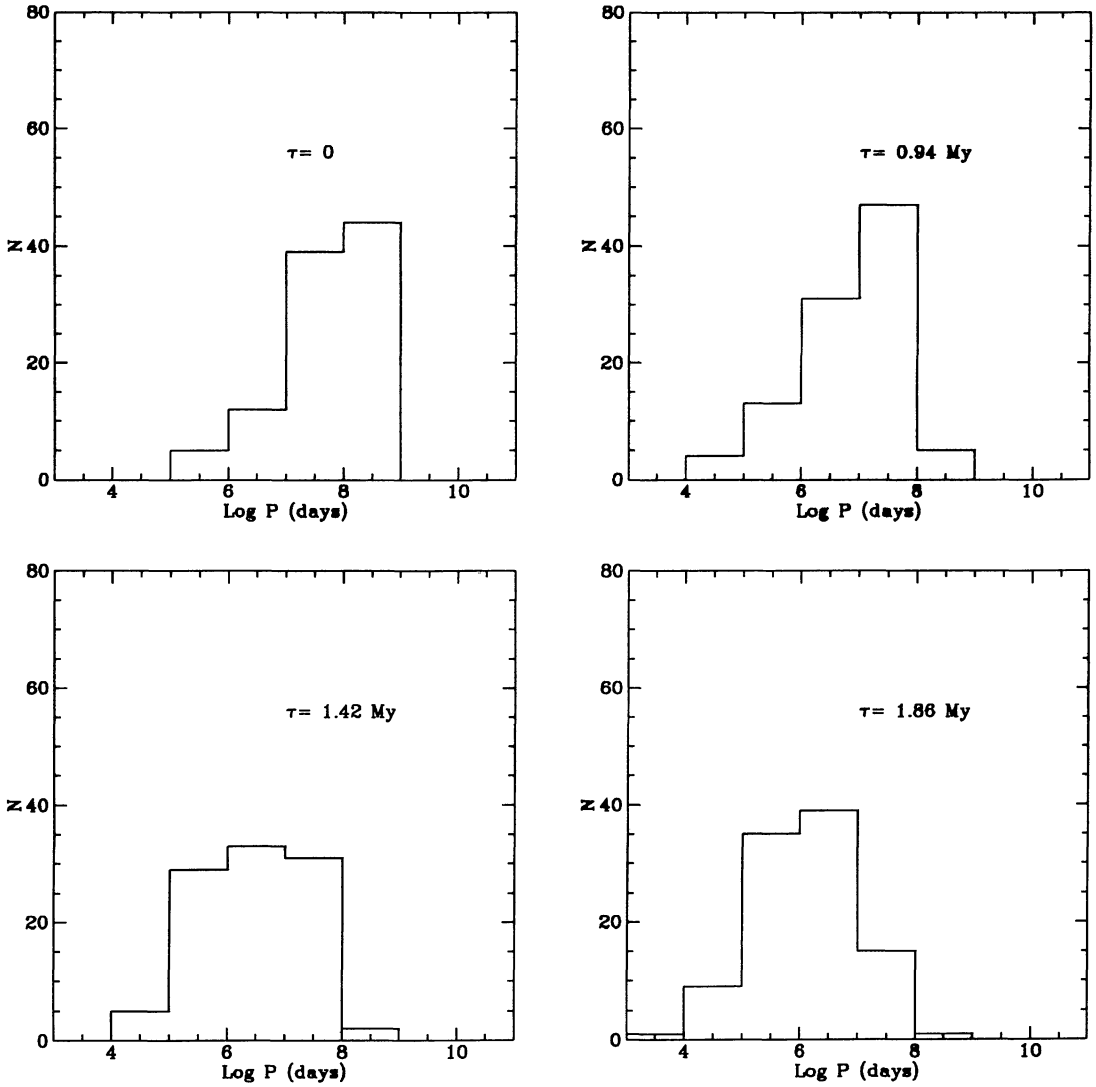

Figure 7. Frequency distribution with periods of binaries which are initially distributed equally in equal intervals of separation. (Case I.)

to smooth out the iregularities, though the precise nature of the resultant frequency distribution would depend on the initial distribution.

7 CONCLUSIONS

The evolution of a protostellar binary system is investigated while it is embedded in its parent molecular cloud core, and is acted upon by gas drag arising from dynamical friction. Approximate analytical results are obtained for the energy and angular momentum evolution of the orbit in the limiting cases, where the velocity is much smaller than, and much larger than the velocity dispersion of the gas. The general case is solved numerically. Dissipation causes a decay of the orbit to smaller separations and orbital eccentricity increases with time. For a protostellar binary embedded in a typical star-forming cloud core (of density $\sim 10^6$ cm^{-3} and a velocity dispersion of 2.3 km s^{-1}) the decay time for the semimajor axis of the orbit to half its initial value is about 10^{5-6} yr. As a binary probably spends about a few 10^6 yr embedded in the cloud, significant evolution of the orbit is expected before the dispersal of the cloud.

Binary populations have been statistically generated and evolved for comparison with observations of MS and PMS binaries. Dynamical friction changes the initial frequency distribution with period of the binaries, and a maximum is obtained in the distribution as seen observationally. Two different initial distributions are considered, and the peak is found to shift slowly towards shorter periods at later times. Decay of the orbit because of gas drag causes an evolution of long-period orbits to shorter periods and thus enables the formation of close binaries.

ACKNOWLEDGMENTS

We thank the referee, Professor R. N. Henriksen, for useful comments.

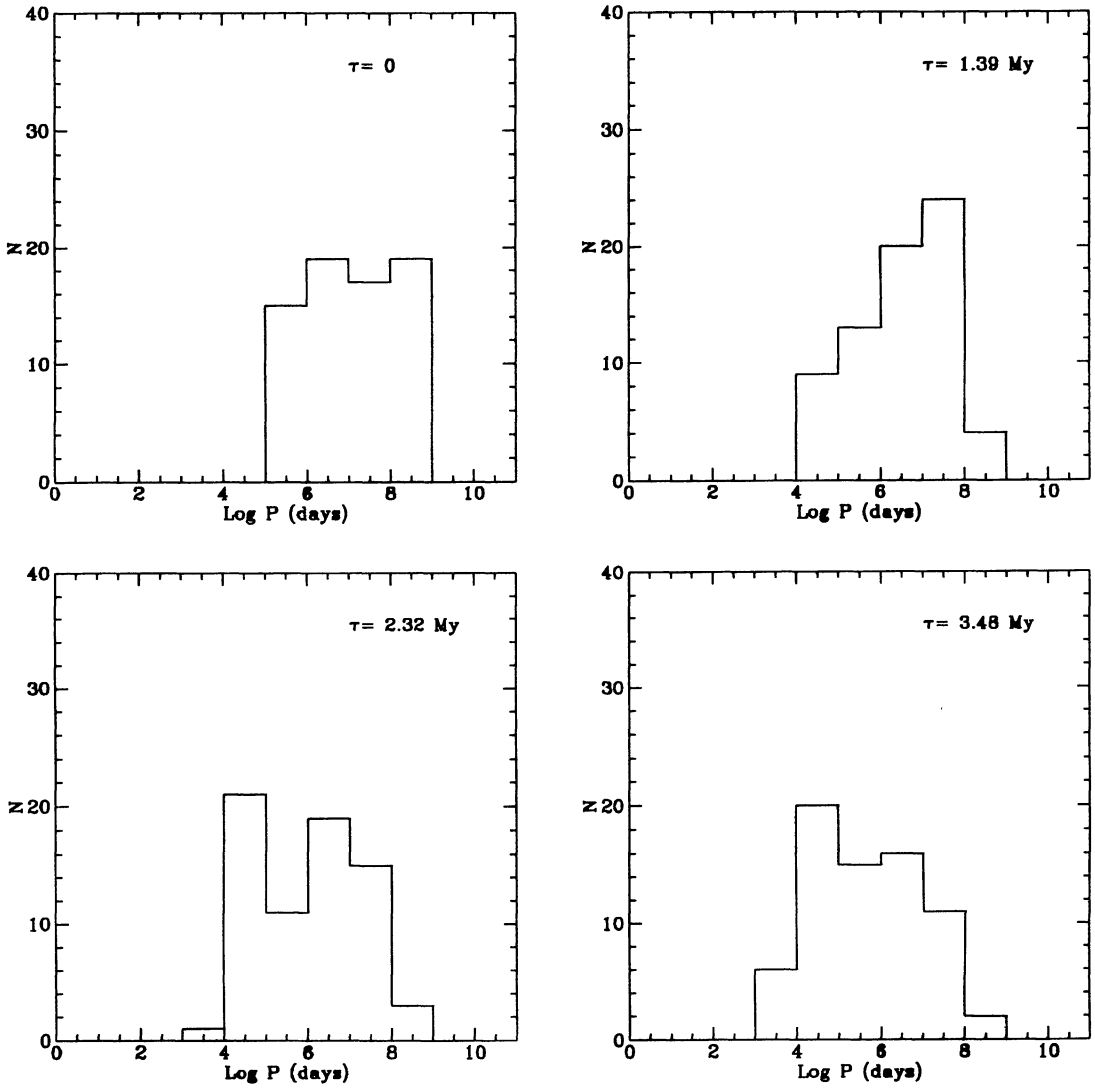

Figure 8. Frequency distribution with periods of binaries which are initially distributed equally in equal logarithmic intervals of separation. (Case II.)

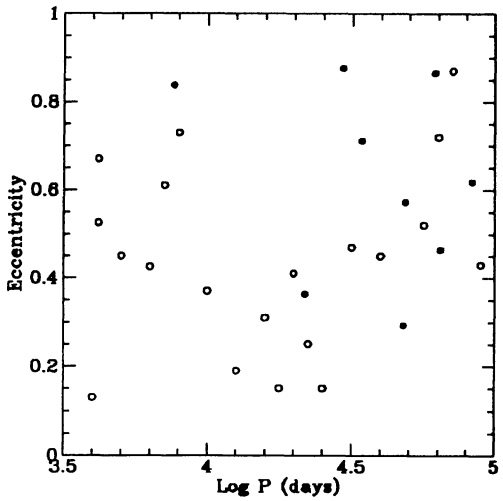

Figure 9. The eccentricity–period distribution for MS binaries (open circles) (from Duquennoy & Mayor 1991) and PMS binaries after 1.8×10^6 yr (filled circles). (Plotted for case I.)

REFERENCES

Abt H. A., 1983, ARA&A, 21, 343
Alexander M. E., Chau W. H., Henriksen R. N., 1976, ApJ, 204, 879
Binney J., Tremaine S., 1987, Galactic dynamics. Princeton Univ. Press, Princeton, p. 791
Bodenheimer P., 1992, in Tenorio-Tagle G., Prieto F., Sánchez F., eds, Star Formation in Stellar Systems. Cambridge Univ. Press, Cambridge, p. 1
Bodenheimer P., Tohline J. E., Black D. C., 1980, ApJ, 242, 209
Boss A. P., 1992, in McAlister H. A., Hartkopf W. I., eds, Proc. IAU Colloq. 135, Complementary approaches to double and multiple star research. Astron. Soc. Pac., San Francisco, p. 195
Chandrasekhar S., 1943, ApJ, 97, 255
Clarke C., 1992, in McAlister H. A., Hartkopf W. I., eds, Proc. IAU Colloq. 135, Complementary approaches to double and multiple star research. Astron. Soc. Pac., San Francisco, p. 176
Duquennoy A., Mayor M., 1991, A&A, 248, 485
Goldstein H., 1977, Classical Mechanics. Addison-Wesley, Amsterdam, p. 24
Henriksen R. N., 1986, ApJ, 310, 189

Henriksen R. N., 1991, ApJ, 377, 500
Hoffer J., 1985, ApJ, 289, 193
Hut P., Makino J., McMillan S., 1995, ApJ, 443, L93
Lienert Ch., Zinnecker H., Weitzel N., Christou J., Ridgeway S., Jameson R., Haas M., Lenzen R., 1993, A&A, 278, 129
Mathieu R. D., 1992, in McAlister H. A., Hartkopf W. I., eds, Proc IAU Colloq. 135, Complementary approaches to double and multiple star research. Astron. Soc. Pac., San Francisco, p. 30
Mathieu R. D., 1994, ARA&A, 32, 465
Pringle J., 1991, in Lada C. J., Kylafis N. D., eds, The physics of star formation and early stellar evolution. Kluwer, Dordrecht, p. 437
Prosser C. F., Stauffer J. R., Hartmann L., Soderblom D. R., Jones B. F., Werner M. W., McCaughrean M. J., 1994, ApJ, 421, 517
Reipurth B., Zinnecker H., 1993, A&A, 278, 81
Shu F. H., Adams F. C., Lizano S., 1987, ARA&A, 25, 23
Strom S. E., Edwards S., Strutskie M., 1992, in Levy E. H., Lunine J. I., eds, Protostars and Planets III. Univ. Arizona Press, Tucson, p. 837